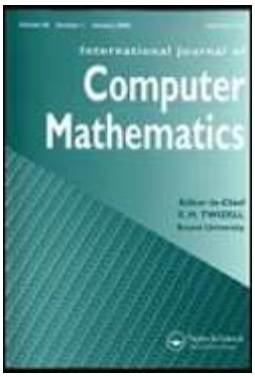

A method of fundamental solutions for two-dimensional heat conduction

Journal:	*International Journal of Computer Mathematics*
Manuscript ID:	GCOM-2009-0885-B.R1
Manuscript Type:	Original Article
Date Submitted by the Author:	28-Jul-2010
Complete List of Authors:	Johansson, B.; University of Birmingham, School of Mathematics Lesnic, D.; University of Leeds, Applied Mathematics Reeve, Thomas; University of Birmingham, School of Mathematics
Keywords:	Heat conduction, Method of fundamental solutions, Regularization, Two-dimensional Domains, Collocation
Note: The following files were submitted by the author for peer review, but cannot be converted to PDF. You must view these files (e.g. movies) online.	
Research paper (2D).zip	

International Journal of Computer Mathematics
Vol. 00, No. 00, January 2008, 1–17

RESEARCH ARTICLE

A method of fundamental solutions for two-dimensional heat conduction

B. Tomas Johansson[a*], Daniel Lesnic[b] and Thomas Reeve[c]

[a,c] *School of Mathematics, University of Birmingham, Birmingham, B15 2TT, UK*;
[b] *Department of Applied Mathematics, University of Leeds, Leeds, LS2 9JT, UK*

(*Received*)

We investigate an application of the method of fundamental solutions (MFS) to heat conduction in two-dimensional bodies, where the thermal diffusivity is piecewise constant. We extend the MFS proposed in [15] for one-dimensional heat conduction with the sources placed outside the space domain of interest, to the two-dimensional setting. Theoretical properties of the method, as well as numerical investigations, are included, showing that accurate results can be obtained efficiently with small computational cost.

Keywords: heat conduction; method of fundamental solutions

AMS Subject Classification: 35K05; 35A35; 65N35

1. Introduction

In many engineering applications finding the solution to various heat conduction problems is of fundamental importance. Examples include, heat exchangers, mathematical finance, in particular after transforming the Black–Scholes equation into the heat equation, and various chemical and biological systems, including diffusion and transportation problems. Thus, due to its importance, many different numerical techniques have been developed for calculating heat flow. The method of fundamental solutions (MFS) is a powerful numerical technique that has been used to obtain highly accurate numerical approximations of solutions to linear partial differential equations (PDEs) with small computational effort, see the reviews [8, 10]. However, this technique has mainly been applied to stationary heat flow governed by elliptic partial differential equations [1, 2]. Recently, in [15], an MFS for the time-dependent linear heat equation in one spatial dimension was proposed and investigated. This method was extended to free surface Stefan problems in [5] and to heat conduction in one-dimensional layered materials in [16]. Encouraged by these results, in this paper we extend the approach considered in [15] to heat conduction in two-dimensional bodies. We note that other formulations of the MFS for the parabolic heat equation were given in [4, 11, 19, 25, 26].

We begin the work in Section 2 by introducing some notation and function spaces, and formulate and review results for the linear heat conduction equation. In Section 3, we prove some theoretical results that we will use in our MFS formulation, in particular, that linear combinations of fundamental solutions are dense in the space

*Corresponding author. Email: B.T.Johansson@bham.ac.uk

ISSN: 0020-7160 print/ISSN 1029-0265 online

DOI: 0020716YYxxxxxxxx
http://www.informaworld.com

of square integrable functions defined on the boundary of the solution domain. In Section 4, we describe the MFS implementation for various (bounded) solution domains. In Section 5, we present numerical results for both some direct problems and also for one inverse problem. These results show that accurate approximations can be obtained efficiently with small computational effort.

2. Preliminaries and notation

We let $\mathbf{x} = (x_1, x_2)$ and $\mathbf{y} = (y_1, y_2)$ be points in $\mathbb{R}^2$ and $T > 0$ be a fixed real number. The conducting body D is a two-dimensional bounded domain in $\mathbb{R}^2$ with smooth bounding surface $\Gamma = \partial D$, for example, C^2-smooth is sufficient. The closure of the body D is $\bar{D} = D \cup \Gamma$. Composed with time we have the following cylinders $D_T = D \times (0, T]$ and $\Gamma_T = \Gamma \times (0, T]$, respectively. The closures of D_T and Γ_T are given by $\bar{D}_T = \bar{D} \times [0, T]$ and $\bar{\Gamma}_T = \Gamma \times [0, T]$, respectively.

We are interested in constructing the solution u to the heat equation in the domain D_T, supplied with initial and Dirichlet boundary conditions, that is u solves

$$\frac{\partial u(\mathbf{x}, t)}{\partial t} - \Delta u(\mathbf{x}, t) = 0, \quad (\mathbf{x}, t) \in D_T, \tag{1}$$

$$u(\mathbf{x}, t) = h(\mathbf{x}, t), \quad (\mathbf{x}, t) \in \Gamma_T, \tag{2}$$

$$u(\mathbf{x}, 0) = u_0(\mathbf{x}), \quad \mathbf{x} \in D, \tag{3}$$

where $u_0(\mathbf{x})$ and $h(\mathbf{x}, t)$ are sufficiently smooth functions. We point out that, in principle, the MFS that we propose and investigate can be applied to other boundary conditions, such as Neumann and mixed boundary conditions.

To guarantee the existence and uniqueness of a solution to (1)–(3) we impose the following compatibility conditions:

$$u_0(\mathbf{x}) = h(\mathbf{x}, 0) \quad \text{and} \quad \frac{\partial h}{\partial t}(\mathbf{x}, 0) = \Delta u_0(\mathbf{x}), \ \mathbf{x} \in \Gamma. \tag{4}$$

With these conditions the following uniqueness theorem holds, see, for example, [9].

THEOREM 2.1 *Let $u_0(\mathbf{x}) \in C^2(\bar{D})$ and $h(\mathbf{x}, t) \in C^1(\bar{\Gamma}_T)$ satisfy the compatibility conditions* (4)*. Then there exists a unique solution $u \in C^{2,1}(\bar{D}_T)$, to the equations* (1)–(3)*, which depends continuously on the data.*

Theorem 2.1 tells us, in particular, that the problem given by the equations (1)–(3) is well-posed.

3. Denseness properties of linear combinations of fundamental solutions

The fundamental solution of (1) in two-dimensions is given by

$$F(\mathbf{x}, t; \mathbf{y}, \tau) = \frac{H(t - \tau)}{4\pi(t - \tau)} e^{-\frac{|\mathbf{x}-\mathbf{y}|^2}{4(t-\tau)}}, \tag{5}$$

where H is the Heaviside function which is introduced in order to emphasize that the fundamental solution is zero for $t \leq \tau$. We shall investigate some properties of linear combinations of such functions for various source points $\mathbf{y}$.

We begin by constructing a set of source points placed outside the region $\bar{D}$. Let D_E (E for enclosed) be an open domain, containing $\bar{D}$, with bounding surface Γ_E, where the distance between the points on the surfaces Γ and Γ_E is greater than zero. Let $\{\mathbf{y}_j, \tau_m\}_{j,m=1,2,\ldots}$ be a denumerable, everywhere dense set of points in $\Gamma_E \times [-T, T]$, $(\tau_m \neq 0)$ and set

$$v_m^{(j)}(\mathbf{x}, t) = F(\mathbf{x}, t; \mathbf{y}_j, \tau_m). \tag{6}$$

Figure 1 shows how the source points may be placed around a domain D, either using a symmetric shape or shapes which take the general shape of Γ obtained by dilatation.

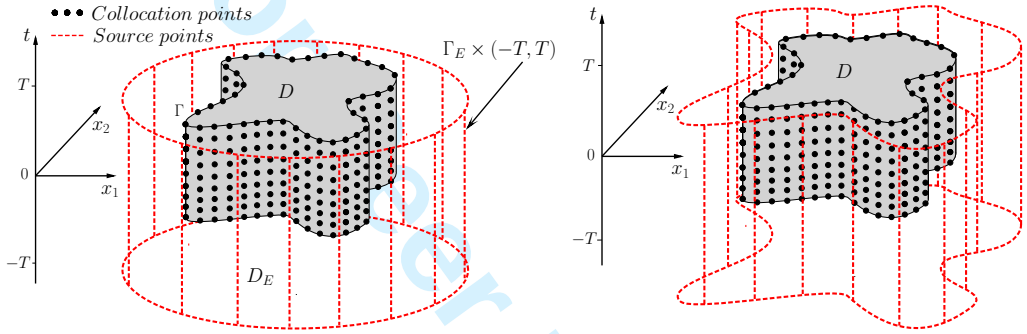

Figure 1. MFS for two-dimensional heat conduction, source points located outside of the spatial domain $\bar{D}$ and in time $[-T, T]$.

We now construct the following infinite series

$$u_\infty(\mathbf{x}, t) = \sum_{j=1}^{\infty} \sum_{m=1}^{\infty} c_m^{(j)} v_m^{(j)}(\mathbf{x}, t), \tag{7}$$

where $c_m^{(j)}$ are set equal to zero except for a finite number of values. Note that, due to the Heaviside function in (5), we have $u_\infty(\mathbf{x}, t) = 0$ for $t \leq \overline{\tau} = \min_{m,j:|c_m^{(j)}| \neq 0} \tau_m$. Also note that, since F solves the heat equation, u_∞ also satisfies the heat equation in D_T.

3.1 *Denseness on the lateral surface*

We prove the following denseness result on the lateral surface $\Gamma \times (-T, T)$:

THEOREM 3.1 *The set of functions* $\{v_m^{(j)}(\mathbf{x}, t)\}_{j,m=1}^{\infty}$ *restricted on* $\Gamma \times (-T, T)$ *form a linearly independent and dense set in* $L^2(\Gamma \times (-T, T))$.

Proof A similar version of the proof of this theorem was given in one-dimension in [15] and in three-dimensions in [21], and we follow those ideas here in the two-dimensional case.

Linear independence: Assume that we do not have linear independence, then there exist positive integers N, $m_0, j_0 \in \{1, \ldots, N\}$, and a coefficient $c_{m_0}^{(j_0)} \neq 0$ such

that

$$\sum_{j=1}^{N}\sum_{m=1}^{N} c_m^{(j)} v_m^{(j)}(\mathbf{x},t) \;=\; 0, \quad (\mathbf{x},t)\in\Gamma\times(-T,T). \tag{8}$$

Define the function

$$U(\mathbf{x},t) \;=\; \sum_{j=1}^{N}\sum_{m=1}^{N} c_m^{(j)} v_m^{(j)}(\mathbf{x},t), \quad (\mathbf{x},t)\in D\times(-T,T). \tag{9}$$

Then U satisfies the following equations:

$$\frac{\partial U}{\partial t} - \Delta U \;=\; 0, \quad \text{in } D\times(-T,T), \tag{10}$$

$$U(\mathbf{x},t) \;=\; 0, \quad (\mathbf{x},t)\in\Gamma\times(-T,T), \tag{11}$$

$$U(\mathbf{x},-T) \;=\; 0. \tag{12}$$

We have obtained the above equations by observing that the fundamental solution satisfies (10); the Heaviside function makes the fundamental solution equal to zero in equation (12), and (8) gives us (11). By the uniqueness Theorem 2.1, the only solution to the equations (10)–(12) is $U(\mathbf{x},t)\equiv 0$ for $(\mathbf{x},t)\in D\times(-T,T)$. Because U is analytic in $D_E\times(-T,T)$, we also have $U(\mathbf{x},t)=0$ for $(\mathbf{x},t)\in D_E\times(-T,T)$, see [24].

We now let the point $(\mathbf{x},t)$ approach the point $(\mathbf{y}_{j_0},\tau_{m_0})\in\Gamma_E\times(-T,T)$ such that the ratio

$$\frac{|\mathbf{x}-\mathbf{y}_{j_0}|^2}{4(t-\tau_{m_0})} \tag{13}$$

remains bounded. Then the summand $c_{m_0}^{(j_0)} v_{m_0}^{(j_0)}(\mathbf{x},t)$ in (8) may be made as large as we wish, while the other terms in the series (8) remain bounded; this gives us a contradiction and thus, we have linear independence for the set of functions $\{v_m^{(j)}(\mathbf{x},t)\}_{j,m=1}^{\infty}$ in $L^2(\Gamma\times(-T,T))$.

Denseness: We next prove that the sequence $\{v_m^{(j)}(\mathbf{x},t)\}_{j,m=1}^{\infty}$ is a dense set in $L^2(\Gamma\times(-T,T))$. Assume on the contrary that it is not a dense set. Then there exists an element $f(\mathbf{x},t)$ in $L^2(\Gamma\times(-T,T))$, which we can assume is continuous, such that

$$\int_{-T}^{T}\int_{\Gamma} v_m^{(j)}(\mathbf{x},t) f(\mathbf{x},t)\,d\mathbf{x}\,dt \;=\; 0, \quad j,m=1,2,\ldots \tag{14}$$

To show that $\{v_m^{(j)}(\mathbf{x},t)\}$ is dense we have to show that $f(\mathbf{x},t)\equiv 0$ in (14). From definition (6), equation (14) can be rewritten as

$$\int_{\tau_m}^{T}\int_{\Gamma} F(\mathbf{x},t;\mathbf{y}_j,\tau_m) f(\mathbf{x},t)\,d\mathbf{x}\,dt \;=\; 0, \quad j,m=1,2,\ldots, \tag{15}$$

where the Heaviside function in (5) has been used to reduce the range of integration with respect to the time variable. We introduce an equivalent form of the classical single-layer heat potential given by

$$V(\mathbf{y},\tau) \;=\; \int_{\tau}^{T}\int_{\Gamma} F(\mathbf{x},t;\mathbf{y},\tau) f(\mathbf{x},t)\, d\mathbf{x}\, dt, \quad \mathbf{y}\notin\Gamma. \tag{16}$$

It is well-known that $V(\mathbf{y},\tau)$ is a smooth solution to the heat equation in the exterior of $\bar{D}\times(-T,T)$ and it cannot vanish on any surface in this exterior region without being identically zero. Thus, by the continuity of F and (15), we find that $V(\mathbf{y},\tau)=0$ for $(\mathbf{y},\tau)\in\Gamma_E\times(-T,T)$, which is in the exterior of $\bar{D}\times(-T,T)$; we then conclude that $V=0$ in the exterior of $\bar{D}\times(-T,T)$. Moreover, since V is continuous across $\Gamma\times[-T,T]$ we also have $V(\mathbf{y},\tau)=0$ on $\Gamma\times[-T,T]$. This implies that $V=0$ also in $\bar{D}\times(-T,T)$ since V satisfies the heat equation in $D\times(-T,T)$. Finally, using the jump relations for the normal derivative of V on $\Gamma\times[-T,T]$, see [9, p. 133], we get

$$\frac{1}{2}f(\mathbf{x},t)\pm\frac{\partial V(\mathbf{x},t)}{\partial\nu} \;=\; 0, \quad (\mathbf{x},t)\in\Gamma\times(-T,T), \tag{17}$$

where ν represents the unit normal on the surface $\Gamma\times(-T,T)$. Thus, $f\equiv 0$ and therefore, $\{v_m^{(j)}(\mathbf{x},t)\}_{j,m=1}^{\infty}$ is a dense set in $L^2(\Gamma\times(-T,T))$. ■

3.2 *Denseness on the base surface*

We now show that we also have denseness on the "base" surface $D\times\{0\}$, where the initial condition is imposed in (1)–(3).

THEOREM 3.2 *The set of functions* $\{v_m^{(j)}(\mathbf{x},0)\}_{j,m=1}^{\infty}$, *where* $v_m^{(j)}(\mathbf{x},t)$ *is given by* (6) *with* $\tau_m<0$, *form a linearly independent and dense set in* $L^2(D)$.

Proof The method of proof is similar to that used in [15] in one-dimension, and we give it here, for completeness, in higher dimensions.

Linear independence: Assume that we do not have linear independence, then there exist positive integers N, $m_0, j_0\in\{1,\ldots,N\}$, and a coefficient $c_{m_0}^{(j_0)}\neq 0$ such that

$$\sum_{j=1}^{N}\sum_{m=1}^{N} c_m^{(j)} v_m^{(j)}(\mathbf{x},0) \;=\; 0, \quad \mathbf{x}\in D. \tag{18}$$

We shall use the corollary of Theorem 3 in [17], which guarantees that if $u(\mathbf{x},t)$ is a smooth solution of the heat equation in $\mathbb{R}^2$ that is bounded by $Be^{\beta|\mathbf{x}|^2}$ and if $u(\mathbf{x},0)=\epsilon$ then, $|u(\mathbf{x},t)|\leq\epsilon$, for $0\leq t\leq T$. From (9) and (18) we have that

$$U(\mathbf{x},0) \;=\; 0, \quad \mathbf{x}\in D. \tag{19}$$

We also have that U satisfies (10) and (12). Now, since $U(x_1,x_2,0)$, where $\mathbf{x}=(x_1,x_2)$, is a real analytic function in each of the variables x_1 and x_2, we find that $U(\mathbf{x},0)=0$ for every $\mathbf{x}\in\mathbb{R}^2$, see [20, p. 14]. Moreover, since each $\tau_m<0$, U is continuous on $\mathbb{R}^2\times[0,T]$ and is at least twice continuously differentiable in $\mathbb{R}^2\times[0,T]$. Furthermore, U also satisfies the heat equation (1), and the following

inequality clearly holds

$$|U(\mathbf{x},t)| \leq Be^{\beta|\mathbf{x}|^2}, \quad t \in [0,T], \tag{20}$$

for some positive constants B and β. Thus, from Theorem 3 of [17], and its corollary, we conclude that $U(\mathbf{x},t) = 0$ in $\mathbb{R}^2 \times [0,T]$. In particular, from [24], we may extend U such that $U(\mathbf{x},t) = 0$ also in $D_E \times [-T,T]$.

We now let the point $(\mathbf{x},t)$ approach the point $(\mathbf{y}_{j_0}, \tau_{m_0}) \in \Gamma_E \times [-T,0]$ such that the ratio (13) remains bounded. Now, the summand $c_{m_0}^{(j_0)} v_{m_0}^{(j_0)}(\mathbf{x},t)$ may be made as large as we wish, while the other terms in the series (18) remain bounded; this gives a contradiction and we have linear independence for the set of functions $\{v_m^{(j)}(\mathbf{x},0)\}$ in $L^2(D)$.

Denseness: We shall show that the set of functions $\{v_m^{(j)}(\mathbf{x},0)\}$, where $\tau_m < 0$, is a dense set in $L^2(D)$. Assume that this is not a dense set, then there exists a function $f \in C^2(D)$ such that

$$\int_D v_m^{(j)}(\mathbf{x},0) f(\mathbf{x})\, d\mathbf{x} = 0, \quad j,m = 1,2,\ldots \tag{21}$$

We let w be a weak solution of the heat equation (1), see [7], with initial condition $w(\mathbf{x},0) = f(\mathbf{x})$ and boundary condition $w(\mathbf{x},t) = 0$ for $(\mathbf{x},t) \in \Gamma_T$. We may transform (21) using Green's identities, see [22], into the following form

$$\int_0^T \int_\Gamma v_m^{(j)}(\mathbf{x},t) \frac{\partial w(\mathbf{x},t)}{\partial \nu}\, d\mathbf{x}dt = 0, \quad j,m = 1,2,\ldots$$

where ν is the outward pointing unit normal to Γ. From Theorem 3.1 we know that $\{v_m^{(j)}(\mathbf{x},t)\}$ restricted on Γ_T is a dense set in $L^2(\Gamma_T)$, and we may conclude that the normal derivative of w is zero on Γ_T. Therefore, both w and $\frac{\partial w}{\partial \nu}$ are zero on Γ_T. From [24], we conclude that $w(\mathbf{x},t) = 0$ for $(\mathbf{x},t) \in \bar{D}_T$; hence $f \equiv 0$, and $\{v_m^{(j)}(\mathbf{x},0)\}$, where $\tau_m < 0$, is a dense set in $L^2(D)$. ■

4. The MFS for the heat equation in two-dimensions

The denseness results proved in the previous section, Theorems 3.1 and 3.2, which involved linear combinations of the fundamental solution (5) of the heat equation (1), enable us to describe a method for approximating the solution to the problem (1)–(3). We note that the MFS we propose may be applied to domains of general shape and size and the source points may also be placed arbitrarily, for example, placed symmetrically on a circular pseudo-boundary, or to match similarly the general shape of the domain D, see Figure 2 and [12]. The only restriction on the placement of the source points is that they are located on the boundary Γ_E outside the domain D, and placed relatively close to D such that u has no singularity in $D_E \times [0,T]$. Also, it might be more practical to take the sources on the interval $(-\epsilon, T)$, where $\epsilon > 0$ is small, instead of the full interval $(-T,T)$. However, some preliminary numerical investigations in [14] for the backward heat conduction problem showed that ϵ cannot be chosen too small if no loss in accuracy and stability is to be secured.

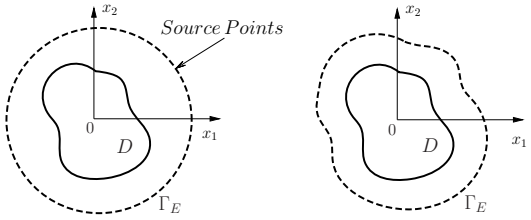

Figure 2. Arbitrary domain with varying source point locations restricted to any contour Γ_E embracing the given solution domain D.

4.1 *A direct MFS for the two-dimensional heat equation*

We search for an approximation to the solution of equations (1)–(3) in the following form:

$$u_{M,N}(\mathbf{x},t) \;=\; \sum_{m=1}^{2M}\sum_{j=1}^{N} c_m^{(j)} F(\mathbf{x},t;\mathbf{y}_j,\tau_m), \quad (\mathbf{x},t)\in \bar{D}_T. \tag{22}$$

For simplicity, let us describe the MFS in the case of circular domains. We shall also consider rectangular domains in the next section, see Example 3 and 4.

We consider a two-dimensional circular domain D, with boundary Γ and radius $r_0 > 0$, centred at the origin, and let us place the source points $(\mathbf{y}_j)_{j=\overline{1,N}}$ on a circle $r_0 + h$, $h > 0$, also centred at the origin. The parameter $h > 0$ will be chosen such that the error at the lateral and base surfaces is minimized (viz maximum principle for the heat equation).

Take the time points $(\tau_m)_{m=\overline{1,2M}}$ (each in the interval $(-T,T)$) as given by

$$\tau_m \;=\; \frac{2(m-M)-1}{2M}T, \;\; m=1,\ldots,2M,$$

and using polar coordinates, place the source points in space at

$$\mathbf{y}_j \;=\; (r_0+h,\theta_j) \;=\; \left(r_0+h,\frac{2\pi j}{N}\right), \;\; j=1,\ldots,N.$$

In polar coordinates equation (22) is now represented by

$$u_{M,N}(r,\theta,t) \;=\; \sum_{m=1}^{2M}\sum_{j=1}^{N} c_m^{(j)} F(r,\theta,t;r_0+h,\theta_j,\tau_m). \tag{23}$$

We have located $N \times 2M$ source points in total outside the domain D and in time; we place the same number of collocation points in total on $\bar{\Gamma}_T \cup (D\times\{0\})$, the boundary in time and the domain at time $t = 0$. Of course, the location of source and collocation points may be chosen arbitrarily, here we choose points for ease of calculation. Let

$$t_i \;=\; \frac{i}{M}T, \;\; i=0,\ldots,M,$$

and on Γ set

$$(r_0,\theta_k) \;=\; \left(r_0,\frac{2\pi k}{N}\right), \;\; k=1,\ldots,N.$$

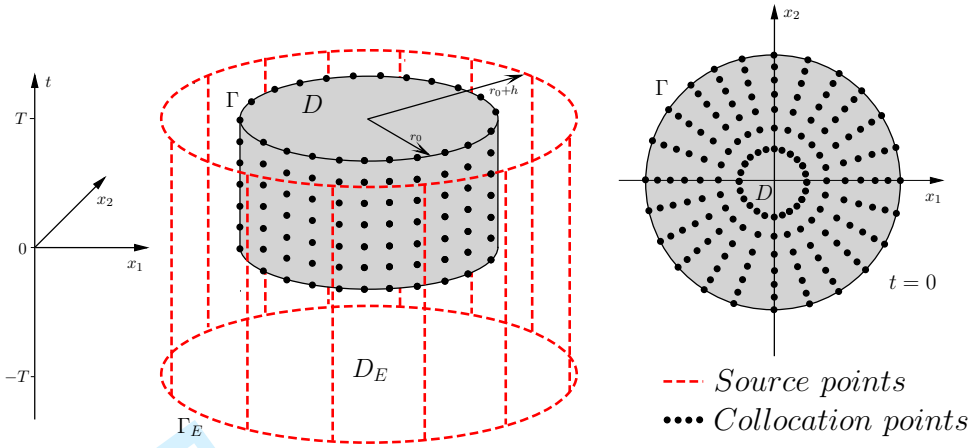

Figure 3. Location of source and collocation points when D is a circular domain.

We have located $N \times (M+1)$ collocation points on the boundary, the remaining $N \times (M-1)$ points will be located on D when $t = 0$. We consider $M-1$ circles of radius

$$r_l = \left(\frac{l}{M}\right)^{\frac{1}{2}} r_0, \quad l = 1, \ldots, M-1,$$

where the square root has been introduced to spread the points out within the domain, and not to cluster them at the centre. We place N equally spaced points on each circle such that

$$(r_l, \theta_k) = \left(r_l, \frac{2\pi k}{N}\right), \quad k = 1, \ldots, N,$$

see Figure 3 for a detailed graphical representation of the position of the various source and collocation points given above.

We now impose the boundary and initial conditions (2) and (3) so that we can determine the unknown coefficients $c_m^{(j)}$ in (23). In polar coordinates we obtain the equations

$$u_{M,N}(r_0, \theta_k, t_i) = h(r_0, \theta_k, t_i), \tag{24}$$

$$u_{M,N}(r_l, \theta_k, 0) = u_0(r_l, \theta_k, 0), \tag{25}$$

where $k = 1, \ldots, N$, $i = 0, \ldots, M$ and $l = 1, \ldots, M-1$.

The system of equations (24) and (25) contains $N \times (M-1) + N \times (M+1) = 2MN$ equations and $2MN$ unknowns, therefore, we may obtain a unique solution. We can represent this system of equations as

$$\mathbf{Ac} = \mathbf{g}, \tag{26}$$

where $\mathbf{c}$ is the vector of unknowns $c_m^{(j)}$, $\mathbf{g}$ is the vector representing the values of the functions u_0 and h at the respective collocation points, and $\mathbf{A}$ is the matrix corresponding to the value of the fundamental solution at the points outlined above. For certain boundary collocation and source points it might be possible to use the

properties of circulant matrices to develop a matrix decomposition algorithm [18] for the solution of the system of equations (26) and thus, substantially reduce the computational cost. This could be considered in a future investigation.

To solve this system it is possible to solve it directly by Gaussian elimination. However, it is well-known that employing the MFS can yield matrices with large condition numbers [6, 23], as h increases. Then, in such a situation instead of (26) it may be necessary to consider the Tikhonov regularization

$$(\mathbf{A}^{tr}\mathbf{A} + \lambda\mathbf{I})\mathbf{c} = \mathbf{A}^{tr}\mathbf{g}, \tag{27}$$

where the superscript ^{tr} denotes the transpose of a matrix and $\mathbf{I}$ is the identity matrix. The linear system of equations (27) is solved using a Gaussian elimination method (employed backslash "\" command in MATLAB). In (27), $\lambda > 0$ is a small regularization parameter (usually in the interval $[10^{-1}, 10^{-16}]$) can be chosen by trial and error, namely start with a large value of λ, say $\lambda = 10^{-1}$, and then decrease it gradually as $\lambda = 10^{-2}, 10^{-3}, \ldots$ until an oscillatory solution starts to develop. To choose λ one can also use the L-curve criterion of [13]. In a future study, it would be interesting to investigate the dependence of the solution on λ and h.

5. Numerical results

In [15] it was shown that the direct MFS approximation applied to the one-dimensional heat equation with source points located outside the domain and in time is accurate. Below, we present numerical results for approximations in two-dimensional domains, such as circular and square domains. In order to assess the accuracy of the numerical MFS solutions we compare them with the available exact solutions for various benchmark test examples. Numerical results are presented for $N = 20$ and $M = 30$ points, which were found sufficiently large to ensure that any further increase in these numbers did not significantly improve the accuracy of the numerical solution without affecting its stability.

5.1 *Example 1*

Let $D = \{\mathbf{x} : |\mathbf{x}|^2 < 1\}$, $D_T = \{(\mathbf{x}, t) : |\mathbf{x}|^2 < 1, t \in (0, 1]\}$, and $\Gamma_T = \{(\mathbf{x}, t) : |\mathbf{x}|^2 = 1, t \in (0, 1]\}$. We solve the following problem, using the direct MFS laid out in the previous section,

$$\frac{\partial u(\mathbf{x}, t)}{\partial t} - \Delta u(\mathbf{x}, t) = 0, \quad (\mathbf{x}, t) \in D_T, \tag{28}$$

$$u(\mathbf{x}, t) = 4t + 1, \quad (\mathbf{x}, t) \in \Gamma, \tag{29}$$

$$u(\mathbf{x}, 0) = |\mathbf{x}|^2, \quad \mathbf{x} \in D. \tag{30}$$

The exact solution of problem (28)–(30) is $u(\mathbf{x}, t) = 4t + |\mathbf{x}|^2$. The source points are placed on a circle with radius $1 + h$. The value of $h > 0$ will be chosen appropriately. However, the accuracy of the approximation appears to decrease when $h < 0.25$ or $h > 4$. In Figure 4 the exact solution and the MFS approximations are plotted in one-dimension, $\mathbf{x} = (x_1, 0)$, for times $t \in \{0.2, 0.8\}$ with $\lambda = 10^{-8}$ in the

Tikhonov regularization. As can be seen in Figure 4 the approximation obtained is accurate, and was stable even when considering other small positive values of λ, however, for stable results we could not take $\lambda = 0$ due to the round-off precision errors.

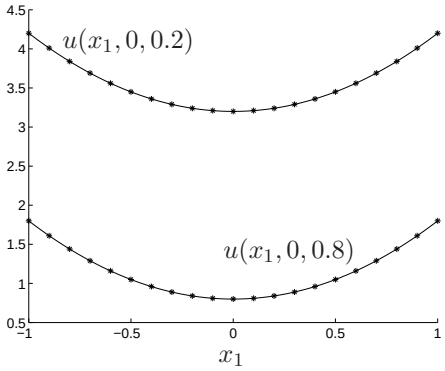

Figure 4. The exact solution (—) and the approximate values (∗) for $u(x_1, 0, 0.2)$ and $u(x_1, 0, 0.8)$, for Example 1.

Figure 5 contains plots of the exact solution and the direct MFS approximations for $h \in \{0.5, 4\}$ and $\lambda = 10^{-8}$. From this figure it can be seen that the numerical results obtained with $h = 0.5$ are slightly more accurate than those obtained with $h = 4$.

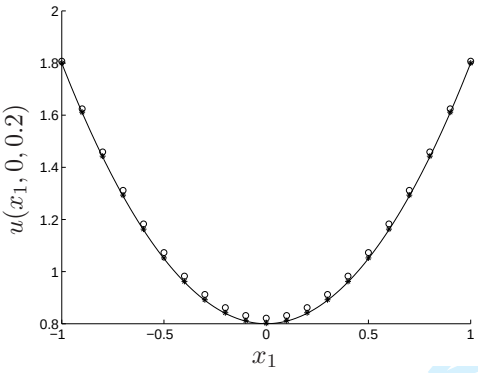

Figure 5. The exact solution (—) and the approximate values for $u(x_1, 0, 0.2)$ obtained with $h = 0.5$ (∗) and $h = 4$ (∘), for Example 1.

Finally, we consider a three-dimensional plot of the exact solution $u(x_1, x_2, 0.8)$ in Figure 6(a), and the MFS approximation $u_{M,N}$ in Figure 6(b) obtained with $h = 1$. Figure 6(c) shows the graph of the absolute error, and we note that the approximation is very accurate with a maximum absolute error of $\mathcal{O}(10^{-5})$.

5.2 *Example 2*

In this example we choose the same D, D_T and Γ as in Example 1, but instead of $u(\mathbf{x}, t) = 4t + |x|^2$, we consider the exact solution of the equations (1)–(3) given by

$$u(\mathbf{x}, t) = e^{x_1 + x_2} \cos(x_1 + x_2 + 4t), \tag{31}$$

where the boundary and initial equations (2) and (3) have been obtained from (31). Note that this function is not constant on circles centred at the origin, and

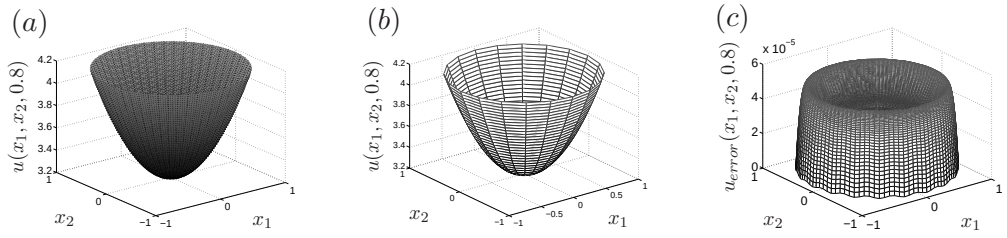

Figure 6. Three-dimensional plot of: (a) The exact solution $u(x_1, x_2, 0.8)$, (b) the approximate solution $u_{M,N}$ obtained with $\lambda = 10^{-8}$ and $h = 1$, and (c) the absolute error, for Example 1.

not symmetric, thus being different in character compared with the solution in Example 1.

Again, the source points will be placed on a circle with radius $1 + h$, with final time point $T = 1$. As an alternative to the strategy for choosing λ described at the end of Section 4.1, we employ the L-curve criterion [13]. In Figure 7 we present a plot of the L-curve for Example 2, where the residual is plotted against the 2-norm of the solution c. We choose the regularization parameter λ, which corresponds to the corner of the "L" in Figure 7; namely, in this example we take $\lambda = 10^{-8}$.

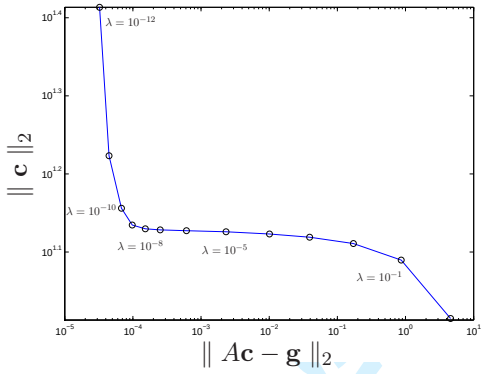

Figure 7. Plot of the L-curve, for Example 2.

In Figure 8 the exact solution and the direct MFS approximations for $\lambda = 10^{-8}$ are plotted in one-dimension, $\mathbf{x} = (x_1, 0)$, for times $t = \{0.2, 0.8\}$, with $h = 1$. It is clear from Figure 8 that the approximation is very accurate. Also, varying λ between $[10^{-12}, 10^{-4}]$ only slightly changes the accuracy of the approximation.

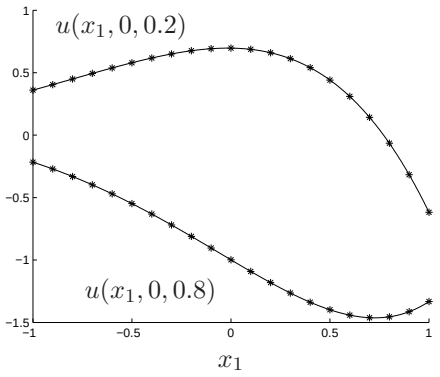

Figure 8. The exact (—) and the approximate values (∗) for $u(x_1, 0, 0.2)$ and $u(x_1, 0, 0.8)$, for Example 2.

Finally, we consider a three-dimensional plot of the exact solution $u(x_1, x_2, 0.8)$

in Figure 9(a), the MFS approximation $u_{M,N}$ in Figure 9(b), and the absolute error in Figure 9(c), obtained with $h = 1$.

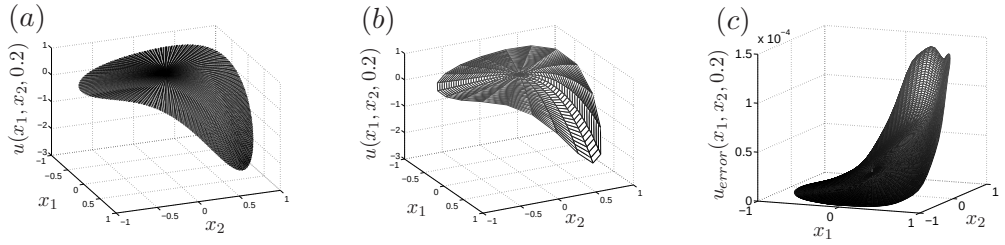

Figure 9. Three-dimensional plot of: (a) The exact solution $u(x_1, x_2, 0.2)$, (b) the approximate solution $u_{M,N}$ obtained with $\lambda = 10^{-8}$ and $h = 1$, and (c) the absolute error, for Example 2.

The plots obtained in Examples 1 and 2 show that the MFS approximation is accurate in circular domains, with errors usually in the interval $[10^{-4}, 10^{-2}]$, for a wide range of parameters h and λ.

5.3 *Example 3*

In the next two examples we consider square domains with edge length L. In Examples 3 and 4 source points will be placed on both squares, see Figure 10, as well as circles; we vary the shapes where we place the source points to highlight that the placement of the source points do not need to follow the shape of Γ. The numerical implementation is the same as in the previous examples, including the placement of the sources and boundary collocation points and their numbers $N = 20$, $M = 30$.

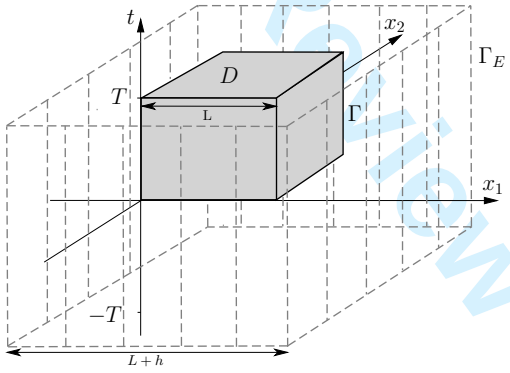

Figure 10. MFS in two-dimensions for square domains.

The following problem was considered in [11]. We take $D = (-0.2, 0.2) \times (-0.2, 0.2)$ to be a square of edge length $L = 0.4$, take $T = 0.9$, and solve

$$\frac{\partial u(\mathbf{x}, t)}{\partial t} - \alpha \Delta u(\mathbf{x}, t) = 0, \quad (\mathbf{x}, t) \in D_T = D \times (0, 0.9], \tag{32}$$

$$u(\mathbf{x}, t) = 0, \quad (\mathbf{x}, t) \in \Gamma_T = \partial D \times (0, 0.9], \tag{33}$$

$$u(\mathbf{x}, 0) = 1, \quad \mathbf{x} \in D. \tag{34}$$

Here, we have thermal diffusivity $\alpha = 1000/5.8$, and the fundamental solution of equation (32) is now given by

$$F(\mathbf{x}, t; \mathbf{y}, \tau) = \frac{H(t-\tau)}{4\pi\alpha(t-\tau)} e^{-\frac{|\mathbf{x}-\mathbf{y}|^2}{4\alpha(t-\tau)}}. \tag{35}$$

We note that in this example the compatibility conditions (4) are violated. The exact solution to the problem (32)–(34) is given by, see Carslaw and Jaeger (1959),

$$u(x_1, x_2, t) = \frac{16}{\pi^2}\left[\sum_{n=0}^{\infty} \frac{(-1)^n}{2n+1} e^{-\alpha(2n+1)^2 t\pi^2/(4(L/2)^2)} \cos\left(\frac{(2n+1)\pi x_1}{2(L/2)}\right)\right] \times \left[\sum_{m=0}^{\infty} \frac{(-1)^m}{2m+1} e^{-\alpha(2m+1)^2 t\pi^2/(4(L/2)^2)} \cos\left(\frac{(2m+1)\pi x_2}{2(L/2)}\right)\right]. \tag{36}$$

However, when we plot the exact (using 100 terms in the series expansion (36)) and the approximate solutions at the point $(x_1, x_2) = (0, 0)$ for time $t \in [0, 0.9]$, with source points placed on a square with edge length $0.4 + h$, $h = 5$, $\lambda = 10^{-8}$, we get a large discrepancy, see Figure 11.

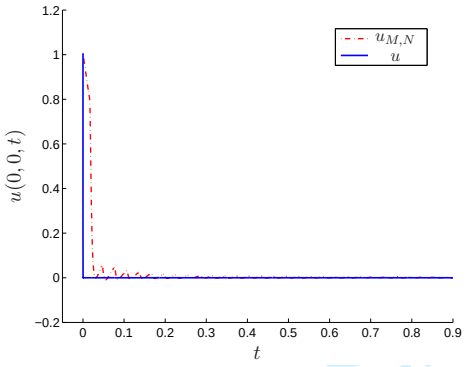

Figure 11. The exact solution $u(0, 0, t)$ and the approximation $u_{M,N}$, as functions of time $t \in [0, 0.9]$, for Example 3.

Changing the parameter λ in the Tikhonov regularization (27) did not seem to improve the approximation, however, we observe that the exact solution (36) decays very rapidly due to the exponential terms. This means that we should consider a much smaller time interval. Figure 12 shows the exact and the approximate solutions, with final time point $T = 0.0006$, plotted over $t \in [0, 0.0004]$, where $\lambda = 10^{-6}$ and source points have now been placed on a circle of radius $h = 0.84$.

These figures show that the choice of the final time T, in particular when considering fast decaying functions, is also important when implementing the MFS. Time-marching methods, [25], could then perhaps be used to extend our approximation to larger time intervals.

5.4 *Example 4*

We consider $D = (0, 1) \times (0, 1)$ and $D_T = D \times (0, 3]$, and we wish to solve the following problem:

$$\frac{\partial u(\mathbf{x}, t)}{\partial t} - \Delta u(\mathbf{x}, t) = 0, \quad (\mathbf{x}, t) \in D_T, \tag{37}$$

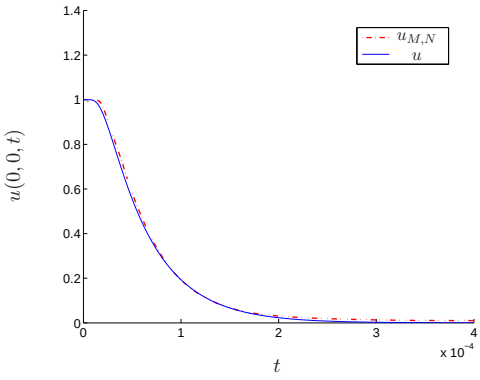

Figure 12. The exact solution $u(0,0,t)$ and the approximation $u_{M,N}$ with $T = 0.0006$, for Example 3.

$$u(x_1,0,t) = u(x_1,1,t) = \sqrt{2}e^{-\pi^2 t/4}\left[\cos\left(\frac{\pi x_1}{2} - \frac{\pi}{4}\right) + \frac{1}{\sqrt{2}}\right], \quad x_1 \in (0,1), t \in (0,3], \tag{38}$$

$$u(0,x_2,t) = \sqrt{2}e^{-\pi^2 t/4}\left[\cos\left(\frac{\pi x_2}{2} - \frac{\pi}{4}\right) + \frac{1}{\sqrt{2}}\right], \quad x_2 \in (0,1), t \in (0,3], \tag{39}$$

$$\frac{\partial u}{\partial x_1}(0,x_2,t) = \frac{\pi}{2}e^{-\pi^2 t/4}, \quad x_2 \in (0,1), t \in (0,3], \tag{40}$$

$$u(x_1,x_2,0) = \sqrt{2}\left[\cos\left(\frac{\pi x_1}{2} - \frac{\pi}{4}\right) + \cos\left(\frac{\pi x_2}{2} - \frac{\pi}{4}\right)\right], \quad (x_1,x_2) \in D. \tag{41}$$

This is an inverse problem with missing boundary data at $x_1 = 1$, which we wish to determine using the Cauchy boundary data over-specification at $x_1 = 0$. The exact solution of problem (37)–(41) is

$$u(x_1,x_2,t) = \sqrt{2}e^{-\pi^2 t/4}\left[\cos\left(\frac{\pi x_1}{2} - \frac{\pi}{4}\right) + \cos\left(\frac{\pi x_2}{2} - \frac{\pi}{4}\right)\right], \quad (\mathbf{x},t) \in D_T. \tag{42}$$

In this example, we shall show results when the source points are placed on squares, as well as when we place them on circles, to show that placement of the sources does not need to follow the shape of the solution domain. When the source points are placed on a square they will be located at $(-h/2, 1+h/2) \times (-h/2, 1+h/2)$, whilst the source points placed on a circle will have radius h with centre at $(0.5, 0.5)$, see Figure 13.

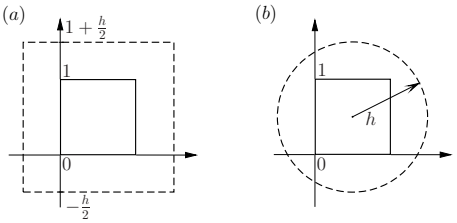

Figure 13. Examples of source point location for the unit square solution domain of Example 4.

Figures 14(a) and 14(b) show the exact solution $u(1, x_2, 1.5)$ and its normal derivative $\frac{\partial u}{\partial x_1}(1, x_2, 1.5)$, respectively, in comparison with the approximate solutions, obtained with $h = 3$ and $\lambda = 10^{-8}$.

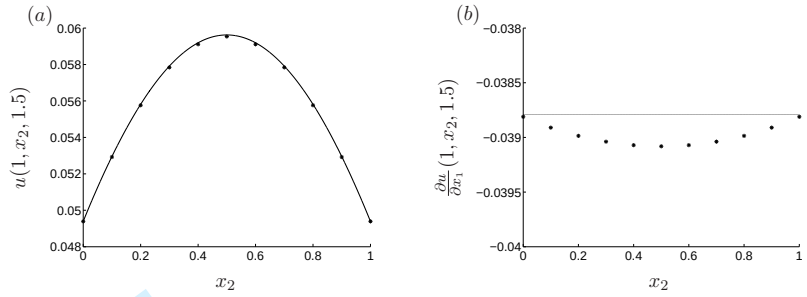

Figure 14. (a) The exact solution $u(1, x_2, 1.5)$ (—) and the MFS approximation $u_{M,N}$ with $h = 3$ ($*$). (b) The exact normal derivative $\frac{\partial u}{\partial x_1}(1, x_2, 1.5)$ (—) and the MFS approximation ($\circ$), for Example 4.

Figure 15 shows the exact solution $u(x_1, x_2, 0.5)$ and the MFS approximation $u_{M,N}$. Note that for the approximation $u_{M,N}$ in Figure 15(c) we have instead placed the source points on a circle and there is still good agreement with the exact solution. In Figure 16 we present plots of the absolute error at time $t = 2.5$ for two different values of h. From this figure it can be seen that the error increases when source points have been placed too close to the boundary.

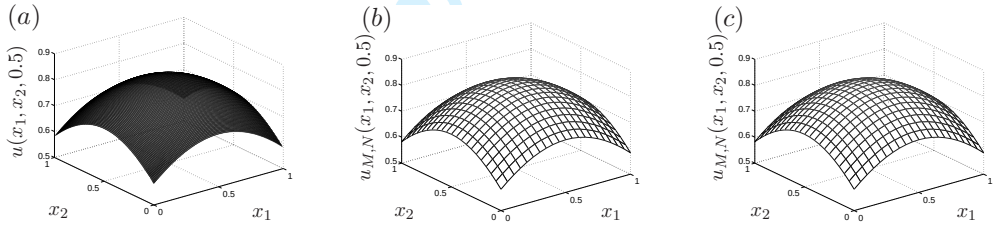

Figure 15. (a) The exact solution $u(x_1, x_2, 0.5)$, (b) the MFS approximation $u_{M,N}$ using source points placed on a square, $h = 3$, and (c) the MFS approximation $u_{M,N}$ using source points placed on a circle with radius $h = 3$ and centre $(0.5, 0.5)$, for Example 4.

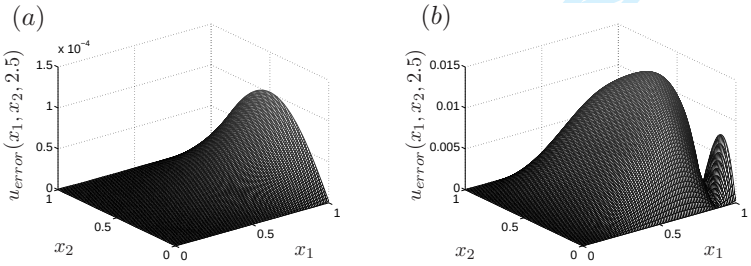

Figure 16. The absolute error $|u(x_1, x_2, 2.5) - u_{M,N}(x_1, x_2, 2.5)|$ when the MFS approximation $u_{M,N}$ has been generated using source points placed on a square with: (a) $h = 3$ and (b) $h = 1$, for Example 4.

Finally, in Figure 17, random noise simulating measurement errors, have been added to the Dirichlet boundary data (39) as follows:

$$u^{\delta}(0, x_2, t) = u(0, x_2, t) + N(0, \sigma^2),$$

where $N(0, \sigma^2)$ represents the normal distribution with mean zero and standard

deviation

$$\sigma = \delta \times \max_{(x_2,t)\in(0,1)\times(0,3)} |u(0, x_2, t)|,$$

and δ is the relative noise level. A set of ten noisy random data functions $\{u_k^\delta(0, x_2, t)\}_{k=\overline{1,10}}$ was generated, and the source points in the MFS have been placed on a circle of radius h, centred at $(1/2, 1/2)$. Figure 17(a) presents a plot of the exact solution $u(1, x_2, 0.5)$, and the best $(*)$ and the least accurate $(\circ)$ MFS approximations from these ten data sets, obtained with $\delta = 3\%$ noise, $h = 3$, $T = 3$ and $\lambda = 10^{-4}$. In Figure 17(b) we present a three-dimensional plot of the absolute error when $\delta = 3\%$, $h = 3$, $\lambda = 10^{-4}$ and $t = 0.5$.

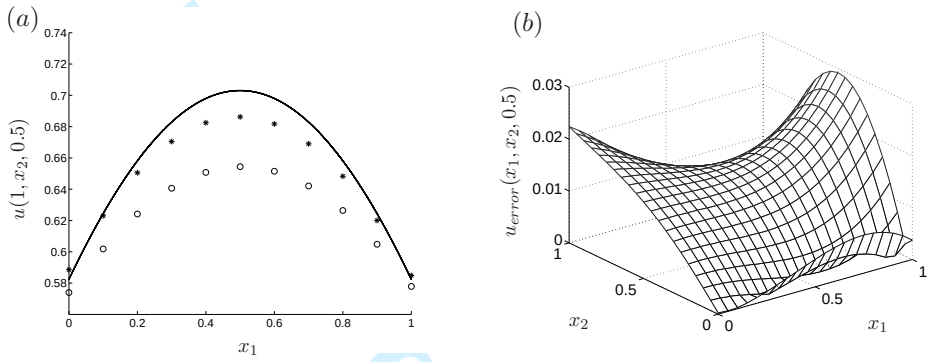

Figure 17. (a) The exact solution $u(1, x_2, 0.5)$ (—) and the best $(*)$ and the least accurate $(\circ)$ MFS approximations from ten different sets of noisy data with noise level $\delta = 3\%$ and (b) the absolute error $|u(x_1, x_2, 0.5) - u_{M,N}(x_1, x_2, 0.5)|$ when $\delta = 3\%$, for one of the noisy data sets, for Example 4.

Adding more noise such as $\delta = 5\%$ did not significantly change the stability of the numerical results provided that regularization is applied appropriately. As expected, the accuracy decreases when the noise level increases and the regularizing parameter usually has to take a larger value. Noise can also be added to the other data functions, such as the Neumann data (40), and the same stable and accurate numerical results are expected. Thus, for this inverse problem, the regularized MFS is a stable approximation with respect to noisy data.

6. Conclusions

We have investigated the application of the MFS for linear heat conduction in two-dimensional conducting bodies with Dirichlet boundary conditions. The solution is sought in the form of a linear combination of fundamental solutions of the heat equation with the source points placed outside the body and in time as well. Theoretical properties, such as denseness of the approximation on the boundary of the body, have been obtained in the space of square integrable functions. Moreover, numerical results are presented for both circular and rectangular configurations showing that accurate approximations can be obtained when the source points are placed on circles or rectangles at an appropriate distance from the solution domain. The numerical results show that accurate approximations can be obtained at small computational cost, and that the method is not too sensitive with respect to the placement of the sources. Numerical results have also been included for an inverse problem, where overspecified data was given on a part of the boundary of a body and the solution was to be reconstructed on the remaining part. Good agreement with the exact available analytical solution was also obtained in this case,

showing that boundary conditions other than Dirichlet can be handled. Extensions to the three-dimensional time-dependent heat equation are straightforward by accordingly modifying the fundamental solution (5).

6.1 *Acknowledgements*

The authors would like to thank the referees for their suggestions. The third author acknowledges financial support from EPSRC in the form of a Doctoral Training Grant (DTG).

References

[1] K. Balakrishnan and P. Ramachandran, *The method of fundamental solutions for linear diffusion-reaction equations*, Math. Computer Modelling 31 (2000), pp. 221–237.
[2] A. Bogomolny, *Fundamental solutions method for elliptic boundary value problems*, SIAM J. Numer. Anal. 22 (1985), pp. 644–669.
[3] H. Carslaw and J. Jaeger, *Conduction of Heat in Solids*, Oxford University Press, London (1959).
[4] S. Chantasiriwan, *Methods of fundamental solutions for time-dependent heat conduction problems*, Int. J. Numer. Meth. Engng. 66 (2006), pp. 147–165.
[5] S. Chantasiriwan, B. Johansson, and D. Lesnic, *The method of fundamental solutions for free surface Stefan problems*, Engng. Anal. Boundary Elements 33 (2009), pp. 529–538.
[6] C. Chen, H. Cho, and M. Golberg, *Some comments on the ill-conditioning of the method of fundamental solutions*, Engng. Anal. Boundary Elements 30 (2006), pp. 405–410.
[7] L. Evans, *Partial Differential Equations*, American Mathematical Society, Providence, Rhode Island (1998).
[8] G. Fairweather and A. Karageorghis, *The method of fundamental solutions for elliptic boundary value problems*, Adv. Comput. Math. 9 (1998), pp. 69–95.
[9] A. Friedman, *Partial Differential Equations of Parabolic Type*, Prentice-Hall Inc., Englewood Cliffs, NJ (1964).
[10] M. Golberg and C. Chen, *The method of fundamental solutions for potential, Helmholtz and diffusion problems*, in *Boundary integral methods: numerical and mathematical aspects*, M. Golberg, ed., Computational Mechanics Publications, Boston (1999), pp. 103–176.
[11] M. Golberg, C. Chen, and A. Muleshkov, *The method of fundamental solutions for time-dependent problems*, in *Proc. 13th Int. Conf. Boundary Element Technology*, C.B. C.S. Chen and D. Pepper, eds., WIT Press, Southampton (1999), pp. 377–386.
[12] P. Gorzelanczyk and J.A. Kolodziej, *Some remarks concerning the shape of the source contour with application of the method of fundamental solutions to elastic torsion of prismatic rods*, Engng. Anal. Boundary Elements 32 (2008), pp. 64–75.
[13] P. Hansen, *Analysis of discrete ill-posed problems by means of the L-curve*, SIAM review 34 (1992), pp. 561–580.
[14] Y. Hon and M. Li, *A discrepancy principle for the source points location in using the MFS for solving the BHCP*, Int. J. Comput. Meth. 6 (2009), pp. 181–197.
[15] B. Johansson and D. Lesnic, *A method of fundamental solutions for transient heat conduction*, Engng. Anal. Boundary Elements 32 (2008), pp. 697–703.
[16] ———, *A method of fundamental solutions for transient heat conduction in layered materials*, Engng. Anal. Boundary Elements 33 (2009), pp. 1362–1367.
[17] R. Johnson, *A Priori Estimates and Unique Continuation Theorems for Second Order Parabolic Equations*, Trans AMS 158 (1971), pp. 167–177.
[18] A. Karageorghis, Y.S. Smyrlis, and G. Fairweather, *Matrix decomposition MFS algorithms*, *International Workshop on MeshFree Methods*, (6 pages).
[19] J. Kolodziej, J. Stefaniak, and M. Kleiber, *Transient heat conduction by boundary collocation methods and FEM - A comparison study*, In: *Notes on Numerical Fluid Mechanics*, pp. 104-115, Braunschweig, Vieweg Verlag (1995).
[20] S. Krantz and H. Parks, *A primer of real analytic functions*, 2nd ed., Birkhauser, Boston (2002).
[21] V. Kupradze, *A method for the approximate solution of limiting problems in mathematical physics*, USSR Comput. Maths. Math. Phys. 4 (1964), pp. 199–205.
[22] J.L. Lions and E. Magenes, *Non-homogeneous Boundary Value Problems and Applications*, vol. 1, Springer, Berlin (1972).
[23] P. Ramachandran, *Method of fundamental solutions: singular value decomposition analysis*, Commun. Numer. Methods Engng. 18 (2002), pp. 789–801.
[24] J.C. Saut and B. Scheurer, *Unique continuation for some evolution equations*, J. differential equations 66 (1987), pp. 118–139.
[25] S. Valtchev and N. Roberty, *A time-marching MFS scheme for heat conduction problems*, Engng. Anal. Boundary Elements 32 (2008), pp. 480–493.
[26] D. Young, C. Tsai, K. Murugesan, and C. Fan, *Time-dependent fundamental solutions for homogeneous diffusion problems*, Engng. Anal. Boundary Elements 28 (2004), pp. 1463–1473.